

Research Article

Fuel Efficiency by Coasting in the Vehicle

Payman Shakouri,¹ Andrzej Ordys,¹ Paul Darnell,² and Peter Kavanagh²

¹ School of Mechanical and Automotive Engineering, Kingston University of London, London SW15 3DW, UK

² Jaguar Land Rover, Banbury Road, Gaydon, Warwickshire CV35 0RR, UK

Correspondence should be addressed to Payman Shakouri; paymash2006@yahoo.com

Received 19 March 2013; Accepted 4 July 2013

Academic Editor: Rakesh Mishra

Copyright © 2013 Payman Shakouri et al. This is an open access article distributed under the Creative Commons Attribution License, which permits unrestricted use, distribution, and reproduction in any medium, provided the original work is properly cited.

This paper investigates the possibility of improving the fuel efficiency by decreasing the engine speed during the coasting phase of the vehicle. The proposed approach is stimulated by the fact that the engine losses increase with the engine speed. If the engine speed is retained low, the engine losses will be reduced and subsequently the tractive torque will be increased, enabling the vehicle to remain moving for longer duration while coasting. By increasing the time period of the coasting the fuel efficiency can be increased, especially travelling downhill, since it can benefit from the kinematic energy stored in the vehicle to continue coasting for a longer duration. It is already industry standard practice to cut fuel during coasting and refuel at low engine speed. The substantial difference proposed in this paper is the controlled reduction of engine speed during this phase and thus reduction in the engine losses, resulting in improved fuel economy. The simulation model is tested and the results illustrating an improvement to the fuel efficiency through the proposed method are presented. Some results of the experimental tests with a real vehicle through the proposed strategy are also presented in the paper.

1. Introduction

Fuel efficiency has been widely researched in the literature from different aspects. Barrand and Bokar [1], Tarpinian et al. [2] have investigated the influence of tyre rolling resistance on fuel saving. Lee et al. [3] have investigated the fuel efficiency through the powertrain and explained that it can be improved by almost locking up the torque converter clutch (TCC) when the vehicle is in coasting. The reason is that energy efficiency can increase up to 100% due to eliminating the slip between the turbine and the impeller. However, if the torque converter is fully locked-up at high speed and the driver lifts the foot from the accelerator pedal, the engine torque suddenly will fall to zero which causes the driver to feel the momentary shock at the moment of lift-up. Thus, the latter paper has proposed an adaptive antishock coasting control to reduce the shock without degrading the fuel economy. Another approach which is commonly used in Hybrid Electric Vehicle (HEV) is the engine start/stop system [4]. Based on this approach, the engine fuelling can be cut off when the engine operates in idle speed. This approach is significantly beneficial

for the vehicle in coasting, because fuelling the engine can be stopped during the coast phase of the vehicle. Lee [4] has studied the benefit of applying the “burn and coast” method in the fuel consumption. According to this method, the vehicle accelerates to the high velocity and then coasts to the lower velocity with the engine off instead of driving at the steady velocity. The “burn and coast” technique is significantly useful for HEV [5–8], because through this technique the vehicle can store high electric energy in the battery during the coast. Some other advanced autonomous systems have been introduced in the literature to control the vehicle speed with respect to the road grade such as Look Ahead Cruise Controller [9–12]. Furthermore, because the engine needs to use higher power to accelerate to high velocity in a short time, the engine brake thermal efficiency is increased. On contrary to [3] which has stated that the greatest fuel efficiency could be achieved by fully locking-up the torque converter, in this paper it has been demonstrated through the simulation that the fuel efficiency can be increased by controlling the slip between the components of the torque converter, that is, the impeller and turbine, through the torque converter slip

control when the vehicle is in the coast phase. Based on the approach proposed in this paper, the coasting duration can be increased by reducing the friction losses in the engine, which requires that the torque converter get unlocked whenever the accelerator pedal is not applied (revised condition), even if the vehicle travels at higher speed. In normal condition, the torque converter is locked at higher vehicle speed about 40 mph (approximately 64.4 km/h) which is equivalent to the third or fourth gear of the transmission. While utilising the revised algorithm the engine can get disengaged from the rest of powertrain, and torque coming to the engine is controlled through the torque converter slip control. In this way, the engine friction losses can decrease which causes fuel efficiency to be improved. The vehicle equipped with revised algorithm can use the potential energy stored during driving downhill so as to increase the coasting duration. In addition, it is proposed that the engine fuelling must be stopped at high vehicle speed during the coasting and the engine must be refuelled at lower vehicle velocity in order to provide further improvement to the coasting duration. Since, at the lower vehicle speed, the torque backed to the engine from the road wheel is not adequate to keep the engine rotating (at engine idle speed), it is crucial to refuel the engine when the vehicle coasts to lower velocity (lower than 15 km/h) such that the engine idle speed can be maintained. Therefore, according to the method proposed in this paper, the engine speed is initially retained at idle level through the torque converter slip control while fuel is cut off, and when the vehicle velocity decreases to 15 km/h, fuelling is started.

Muller et al. [13] propose Stop/Start Coasting, that is, the Bosch concept, in which the fuel injection is turned off during the coasting; however, the combustion engine must be decoupled from the powertrain by opening the clutch or shifting into neutral gear in order to avoid negative engine torque during coasting. Disconnecting the engine from the powertrain, while turning off the fuel injection, prevents the engine from rotating. It has disadvantages as an additional power supply is required to supply systems such as power steering or air conditioning during the coasting condition. The concept proposed in this paper, that is, the Jaguar Land Rover (JLR) concept, is based on the controlled reduction of engine speed through the torque converter slip control during the coasting phase, and thus reduction in the engine frictional and pumping losses, resulting in less drag on vehicle and improved fuel economy over the conventional cases. In this way, unlike the Bosch concept, the combustion engine is not entirely disconnected from the powertrain and can be remained rotated at idle speed through the torque backed to the engine from the road wheels.

This paper is organized as follows. The longitudinal vehicle model is explained in Section 2. Section 3 proposes a new approach for increasing the coasting duration. Section 4 explains the parameters required for measuring fuel consumption and efficiency in the simulation. Section 5 illustrates the simulation results for the coasting and investigates the potential of the fuel efficiency through the approach proposed in this paper. Section 6 presents the results of the real implementation. Finally, Section 7 draws some conclusions and proposes future directions.

2. Vehicle Longitudinal Model

To carry out analysis in this paper, an intergraded simulation model of the vehicle has been developed using Simulink/MATLAB software. The detailed derivation of the vehicle simulation model is presented in the appendix.

The vehicle dynamics is classified into two separate categories [14]: (1) the dynamics of powertrain comprising of the engine, the torque converter, the gear box, the final drive, and the wheels; (2) the dynamics of the vehicle considering the external forces acting on the vehicle. These include aerodynamic drag force, gravitational force, and rolling resistance force.

In the powertrain model, two states of the torque converter, that is, locked and unlocked, are simulated. The transmission between these two states is implemented in the simulation by devising a switching algorithm which depends on the vehicle velocity and the throttle opening position.

The torque converter can get locked up when the vehicle travels at speed higher than 40 mph (approximately 17.88 m/s) or equivalently at third or fourth gear; at this speed the throttle is slightly opened. When torque converter locks up, the impeller and turbine will get entirely engaged so as to provide the one to one drive from the engine to the gear box input shaft without any slippage. Thus, the engine speed will be correlated to the vehicle speed directly through gear and final drive ratios.

In order to take the friction and pumping losses of the engine (for brevity in this paper, these two terms are lumped and denoted by the engine friction) into consideration, a map corresponding to 5-litre naturally aspirated V8 engine (provided by JLR) has been used. This map is illustrated in Figure 1, which introduces the engine friction versus engine rotation speed for the air mass flow of 42%. As it is observed, the engine friction increases along with the engine speed. The engine friction also depends on other characteristics of the engine such as the compression ratio and the engine sizing.

3. Revised Algorithm

When the torque converter enters the lockedup state, the engine speed becomes directly related to the vehicle velocity through gear box and the final drive; therefore the engine speed will remain higher for the longer period of time. An algorithm needs to be devised to prevent the system from staying locked-up during coasting, which can help the engine speed to be reduced promptly. The lower engine speed results in the lower engine friction (see Figure 1). This avoids generating the opposing torque on the wheel due to the engine friction losses during coasting, which consequently helps the vehicle coast for longer duration.

An integrated simulation model of the vehicle dynamics and powertrain considering an automatic transmission and incorporating the unlocked and locked states of the torque converter as well as a switching logic to perform transition between those states is illustrated in Figure 2. In the simulation, it requires two engine models for presenting different conditions of operation: the engine with an unlocked torque converter (Engine 1) and the engine with a locked torque

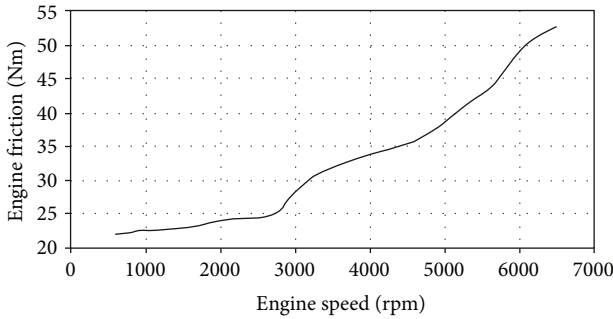


FIGURE 1: The engine friction map for 5-litre naturally aspirated V8 engine.

converter (Engine 2). When the torque converter is unlocked, the operation of system is represented by Engine 1 together with the torque converter model. However, when the torque converter is locked the model does not need to consider the torque converter, since it may be assumed that the engine crank shaft is directly connected to the transmission input shaft. Therefore, the operation of system is only represented by Engine 2, without considering the torque converter. In reality, in our simulation, we use the model which combines those two models together with a switching algorithm (see Figure 2).

In order to investigate the effect of the locked and the unlocked states of the torque converter on the coast duration and fuel efficiency through simulation, an algorithm is presented based on a simple switching algorithm which is triggered by the throttle opening position and the vehicle speed. To investigate the impact of new approach proposed in this paper on the coasting and fuel efficiency, two conditions are, namely, introduced: normal condition and revised condition. During normal condition the switching logic only uses the vehicles velocity in order to transit between locked and unlocked states; regardless of the position of the throttle opening, that is, whether throttle opening is zero or not. In this way the torque converter is locked up when the vehicle travels at speed approximately higher than 17.88 m/s (40 mph) while it is unlocked up at the vehicle speed lower than 17.88 m/s. However, based on the revised condition the torque converter can get unlocked up once the throttle opening position has become zero, even though the vehicle speed is high, which can provide an improvement to the coasting duration. A switching algorithm is utilized in the simulation for performing transition between the locked and unlocked states of the torque converter. Depending on the position of the switches, different values of the engine speed and transmission input torque will be used for the computation. Thus, if either the vehicle velocity is less than 17.88 m/s or the throttle opening is zero (indicating the unlocked state of the torque converter), the engine speed (N_e) calculated by Engine 1 (see Figure 2) and the turbine torque (T_{in1}) calculated by the torque converter model will be used for the engine speed (also as an initial engine speed for the next instance of computation) and transmission input torque (T_{in}), respectively. Otherwise, the transmission input speed (N_{in}) and the torque (T_{in2}) calculated by Engine 2 will be used.

The engine has to be rotated at idle speed during coasting, rather than stopping or rotating fully, to allow ancillary components to operate, that is, power steering, air conditioning, alternator, and so forth and also to improve speed of response should the driver press the accelerator pedal. According to the new concept, the torque converter gets unlocked during coasting and no fuel is injected to the engine. In this condition the engine speed will fall to idle, that is, approximately 610 rpm. In order to keep the engine rotating at the idle speed, the following two approaches can be proposed, depending on the vehicle speed.

3.1. The Torque Converter Slip Control. Based on this new approach, the fuel is not injected into the engine during the coasting phase; thus, the engine speed drops to lower than the idle speed. Therefore, in order to hold the idle engine speed, sufficient connection across the torque converter needs to be generated to provide enough torque back to the engine from the road wheel. This can be achieved through the torque converter slip control.

3.2. Refueling the Engine at Lower Vehicle Speed. At the lower vehicle speed, the torque backed to the engine from the road wheel will not be sufficient to keep the engine rotating at the idle speed. Therefore, it is crucial to refuel the engine when the vehicle coasts to the lower velocity such that the engine idle speed can be maintained. Thereby, refueling the engine at lower vehicle speed provides further improvement on the coasting duration.

To present the two approaches explained above in the simulation, two Proportional-Integral-Derivative (PID) controllers are used. Both controllers try to keep the engine idle speed; one controls the torque coming back to the engine from torque converter, that is, impeller torque, when the vehicle coasts at high speed; other one controls the throttle opening position at low vehicle speed. These algorithms are depicted in Figure 3, which corresponds to the engine model for the unlocked state of the torque converter (Engine 1 depicted in Figure 2).

In the simulation, the torque converter slip control has been virtualized by use of a PID controller (PID controller 1) that controls the impeller torque in order to help the engine speed reach to its set-point. The engine idle speed is introduced as the set-point. Depending on the switching conditions, either the magnitude of the impeller torque calculated by the controller (T_{ic}) or that generated by torque converter (T_i) will be sent to the engine model. The magnitude calculated by the controller (T_{ic}) will be used, if the following three conditions hold at the same time:

- (1) the throttle signal is zero;
- (2) the vehicle velocity is higher than 15 km/h (approximately 4.16 m/s);
- (3) the engine reaches to its idle speed, that is, approximately 610 rpm.

Otherwise the torque generated by the torque converter (T_i) will be used.

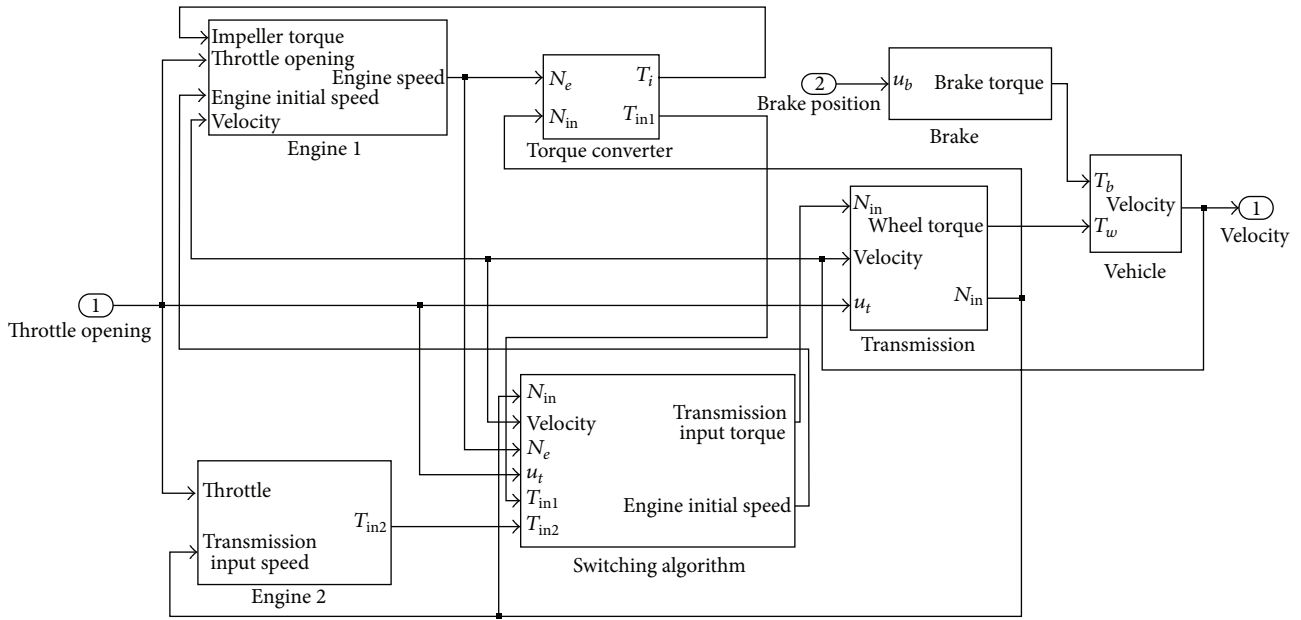


FIGURE 2: An integrated simulation model of the vehicle dynamics and powertrain considering an automatic transmission—both locked and unlocked states of the torque converter are modelled.

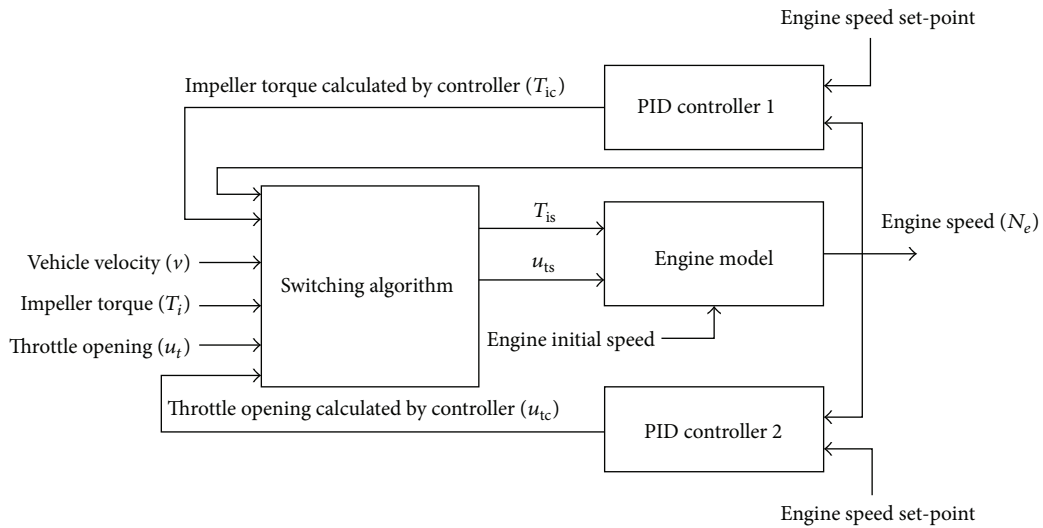


FIGURE 3: Two PID controllers used to keep the idle engine speed (610 rpm) during coasting—the torque backed to the engine from torque converter (impeller torque) is controlled at the higher vehicle speed, while the throttle is controlled to hold the idle engine speed at the lower vehicle speed.

Refueling of the engine at the low vehicle speed is modeled by another PID controller (PID controller 2) which regulates the throttle opening position. The throttle position is adjusted such that the idle engine speed is retained. In this way, the throttle position slightly opens to produce enough torque for keeping the engine at idle speed. Depending on the switching conditions, either the throttle opening magnitude calculated by the controller (u_{ic}) or that predefined as an input to the vehicle simulation model (u_t) will be sent to the engine model. In order for the magnitude calculated by the controller to be used, the following two conditions must hold at the same time:

(1) throttle signal is zero;

(2) the vehicle speed is less than 15 km/h.

Otherwise the pre-defined throttle opening (u_t) will be used.

4. Fuel Efficiency and Fuel Consumption

A term to investigate fuel efficiency is the Brake Specific Fuel Consumption (BSFC). It may be determined by the following equation:

$$BSFC = \frac{\dot{m}_f}{P_{eb}} \tag{1}$$

Here \dot{m}_f denotes fuel consumption rate (g/h) and P_{eb} is engine brake power (kW). To calculate the fuel consumption rate in the simulation, a look-up table giving the brake specific fuel consumption (BSFC) versus brake mean effective pressure bmep (Pa) and engine speed (rpm) is used. The look-up table is not presented in this paper due to the confidentiality issue. The bmep can be calculated from the engine brake torque T_{eb} [15]:

$$\text{bmep} = \frac{n\pi T_{eb}}{V_d}, \quad (2)$$

where V_d denotes the displacement volume of the engine (m^3), n denotes the number of the time the piston moves during one cycle of the engine, that is, the engine stroke, and T_{eb} denotes the engine brake torque (Nm).

5. Simulation Results

The vehicle used for illustration of the proposed approach (through simulation) is a Range Rover Sport L320 with 5-litre naturally aspirated V8 engine including a ZF HP28 six-speed automatic transmission (Figure 4). Hence, the appropriate engine map (provided by JLR) has been used. The torque converter data was obtained from the literature [3].

The simulation results and the results based on the real test data are compared to establish that the dynamics of the vehicle during coasting has correctly been simulated. The real data was collected as follows: the vehicle was driven to 135 km/h on the flat road and neutral gear was selected with the vehicle allowed to coast with no steering input down to 15 km/h. Recording of the data was started from 125 km/h. In order to resemble the same scenario in the simulation, a cruise control (CC) model [16] is utilized to get the engine speed and vehicle velocity to the initial conditions required for the test; thus, the set-point speed of 34.72 m/s (125 km/h) is chosen. Furthermore, for determining the neutral gear in the powertrain model, a simple switch is used to set the gear box output torque, that is, final drive input torque, at zero. In this condition, there is no torque transmission from the engine to the wheel. The comparison results between the simulation and real test data are illustrated in Figure 5. The simulation results are almost identical with the real test data. This indicates that dynamics of the vehicle during coasting is correctly presented by the simulation model.

As it was explained, in normal condition, the torque converter only unlocks up when the speed is less than 64.4 km/h (40 mph). However, according to the new approach the torque converter can get unlocked up whenever the throttle is closed regardless of the vehicle speed. It helps the engine speed decrease faster which in turn reduces the engine friction and the fuel efficiency can be obtained. In order to investigate the influence of the revised algorithm on the coasting duration along with fuel efficiency two scenarios based on the road condition are determined: flat road and inclined road. These two scenarios are presented as follows.

First scenario considers the flat road. For this test, the cruise control (CC) is initially used to make the vehicle velocity track the reference velocity set at 144 km/h. The



FIGURE 4: Range Rover Sport L320 with 5-Litre naturally aspirated V8 engine including a ZF HP28 six-speed automatic transmission.

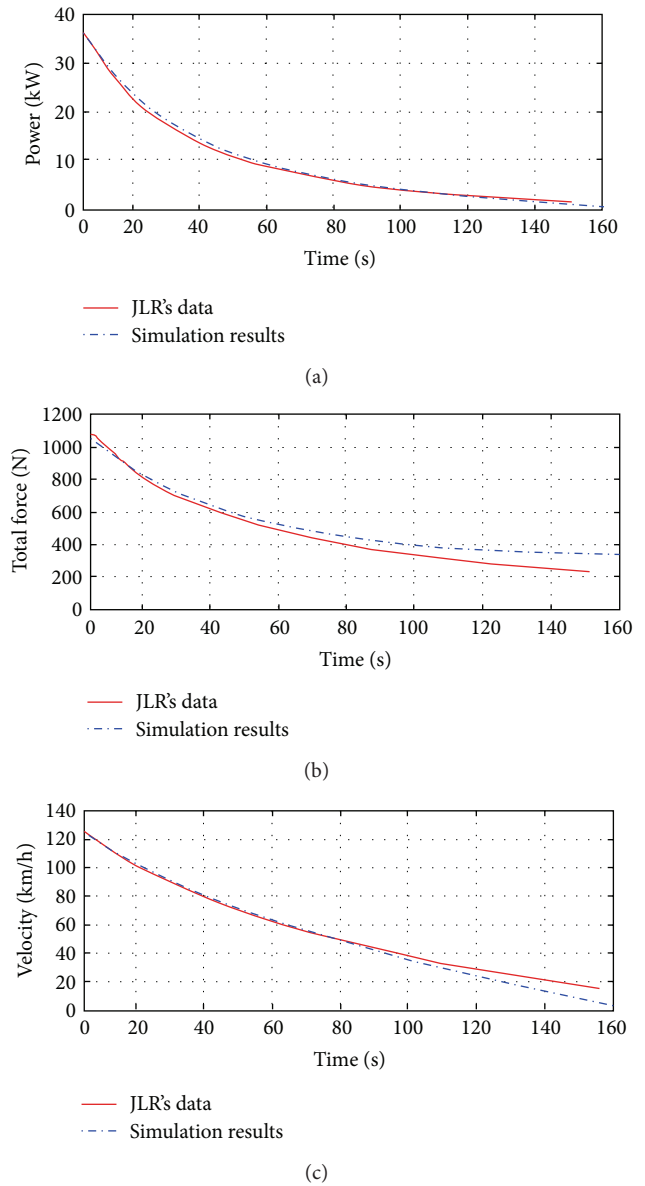


FIGURE 5: (a) Total amount of the external forces acting on the vehicle during coasting—the result of the simulation compared with data obtained from the test on a real vehicle, (b) power presents the reduction of the stored energy over the time as the vehicle coasts down, and (c) comparison of the vehicle's velocities obtained from the simulation model and from the test vehicle.

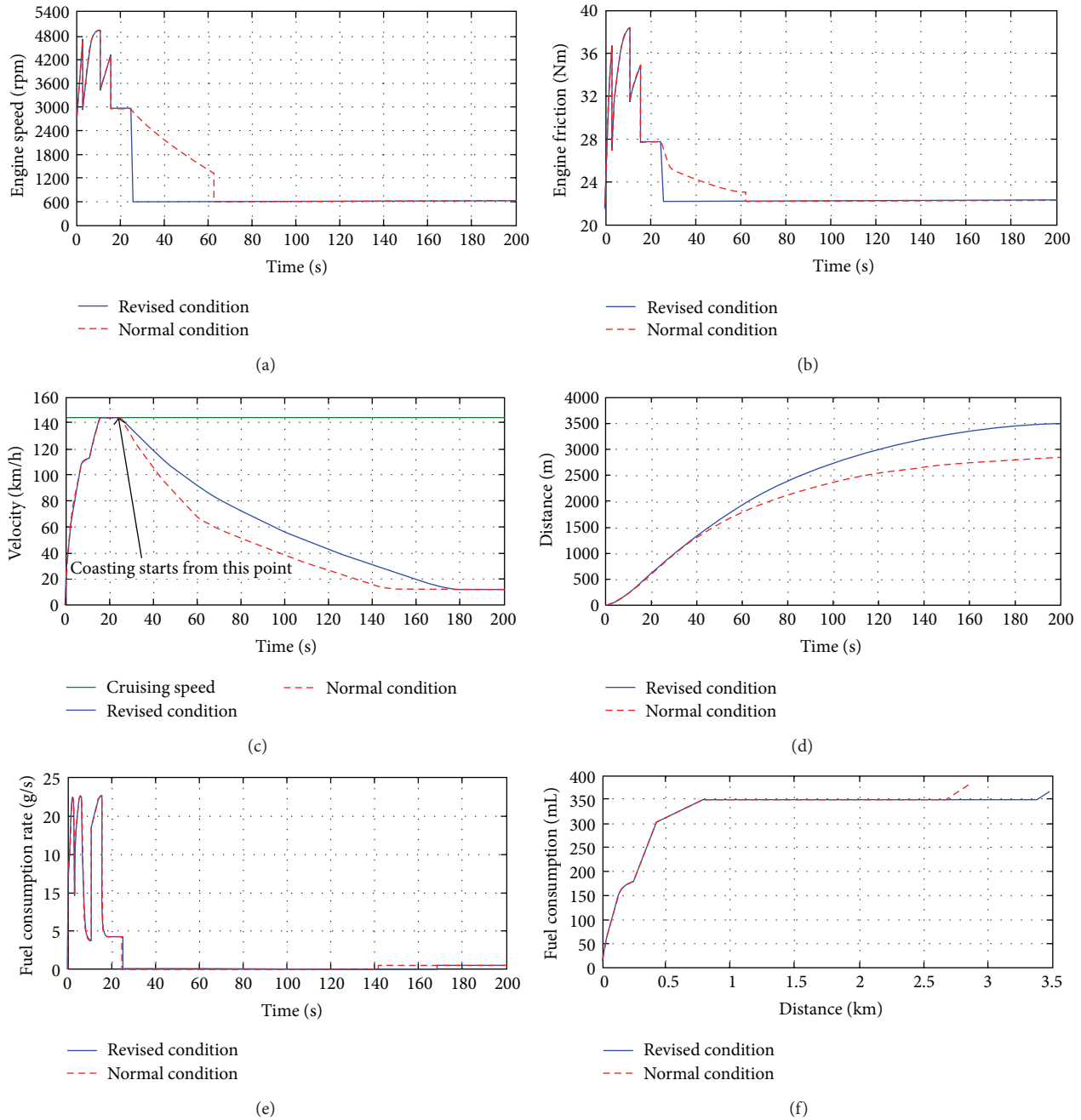


FIGURE 6: (a) The engine speed obtained for the normal and revised conditions—the lower engine speed obtained by the revised algorithm. (b) The engine friction obtained for two conditions—the amount of friction losses is lower via revised algorithm. (c) Vehicle velocity during coasting—longer coasting duration achieved through the revised algorithm. (d) Longer distance covered by the revised algorithm during coasting. (e) Comparison of the fuel consumption rates. (f) Fuel consumption versus distance for two conditions.

CC is switched off to set both the brake and the throttle inputs at zero and to let the vehicle coast, which happens after 25 s. During the normal condition the torque converter stays lockedup at the speed higher than 64.4 km/h resulting in high engine speed (Figure 6(a)) and consequently higher engine friction (Figure 6(b)). High engine friction reduces the overall tractive force which causes the reduction of the coasting duration. However, the revised algorithm does not allow the torque converter to remain lockedup and helping

the engine speed to be reduced quicker, hence longer coasting duration (Figure 6(c)) and coasting distance (Figure 6(d)) can be achieved. The comparisons between two conditions (revised and normal conditions) are illustrated in Figure 6. When using revised algorithm, the torque converter gets unlocked and stays at this state after 25 s, while without the revised algorithm (normal condition) the torque converter stays unlocked between 25 and 62 s and becomes unlocked after 62 s onward. When the vehicle is coasting, no fuel is

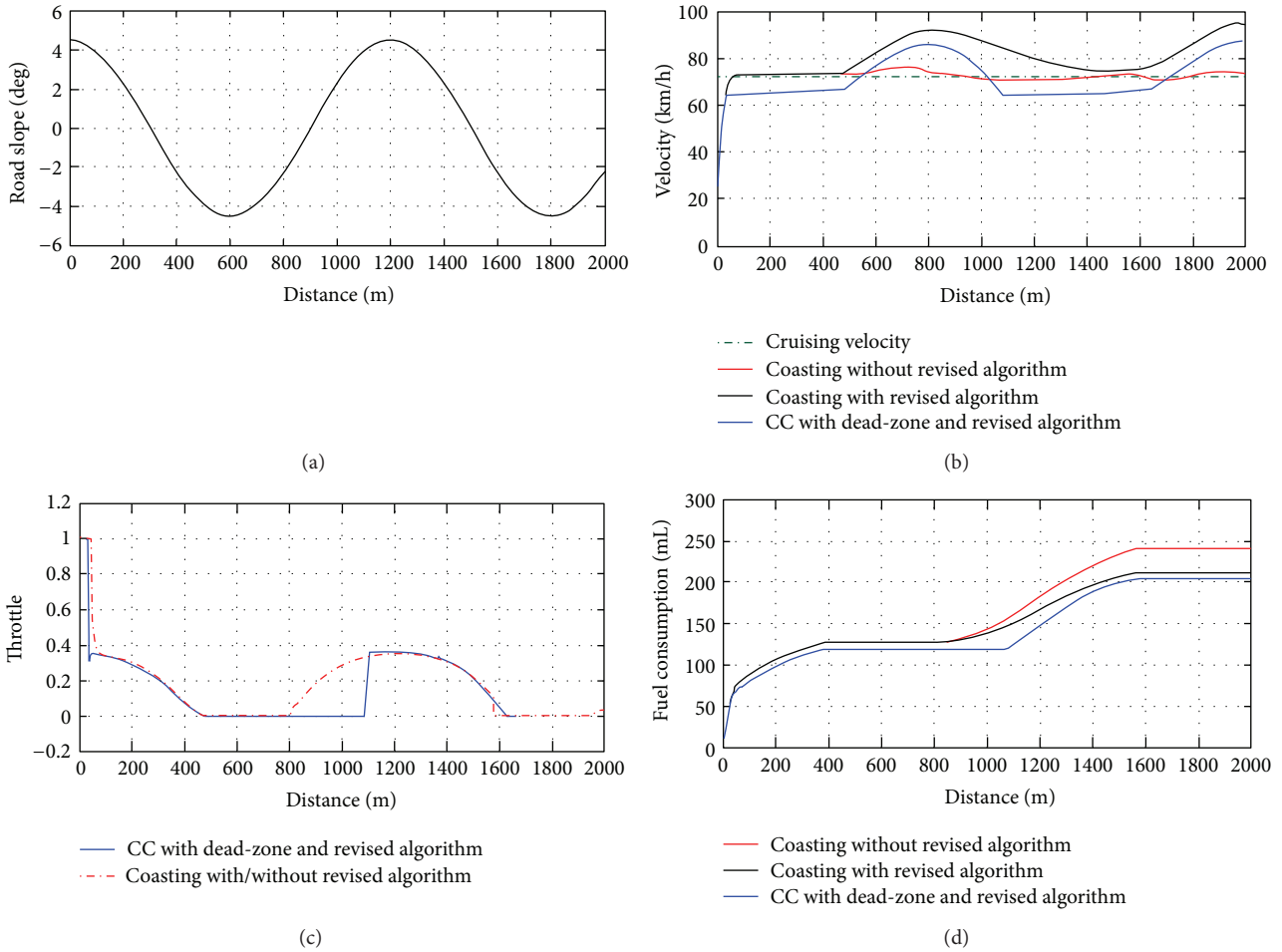


FIGURE 7: The influence of revised algorithm on both fuel consumption and travelled distance is investigated on the inclined road by introducing a simulated road profile (sinusoidal inclination)—(a) road slope. (b) Vehicle velocity. (c) Throttle opening positions. and (d) fuel consumption.

injected into the engine as it is shown in Figure 6(e). But once the vehicle slows down to the speed of approximately 15 km/h, the engine starts being refueled so as to keep it rotating at the idle speed (Figure 6(a)). The time instance when the fuel injection is restarted would be different for the normal and the revised conditions (Figure 6(e)). Figure 6(e) illustrates that the refueling starts at 140 s for normal condition, while it occurs at about 165 s for revised condition. It is due to the vehicle slows down faster in the normal condition (Figure 6(c)). The results demonstrate (Figure 6(f)) that fuel consumption can be reduced about 7.9% through the proposed approach. By consuming the same amount of fuel in both conditions, revised and normal conditions, the travelled distance (Figure 6(d)) could increase about 17.14% through the longer coast duration.

It is believed that the most fuel economy saving can be obtained when the vehicle travels downhill. Thus, the next set of two scenarios (scenarios 1 and 2) is determined to test the new approach (revised algorithm) on the inclined road. The two following tests are carried out:

- (i) simulated road profile (sinusoidal inclination),

- (ii) real road profile, which is used to emulate a real-world driving condition.

Those tests are explained as follows.

5.1. Simulated Road Profile (Sinusoidal Inclination). Three scenarios are defined here to evaluate the fuel efficiency gained through the new approach (Figure 7) for the described road profile, which is based on the sinusoidal variation of the road slope as shown in Figure 7(a). This test is carried out for the three following cases.

5.1.1. Coasting without Revised Algorithm. The test is started with applying the cruise control (CC) algorithm to the road profile illustrated by the road slope in Figure 7(a), so as to maintain the constant speed (72 km/h) as shown in Figure 7(b) after applying CC algorithm and analyzing the results, it is realized that in this particular case the brake is almost zero and braking is not essential. Therefore, it is decided not to consider the brake, especially that the brake is not important from the point of view of fuel consumption. Thus, the CC algorithm is run with the brake set at zero and

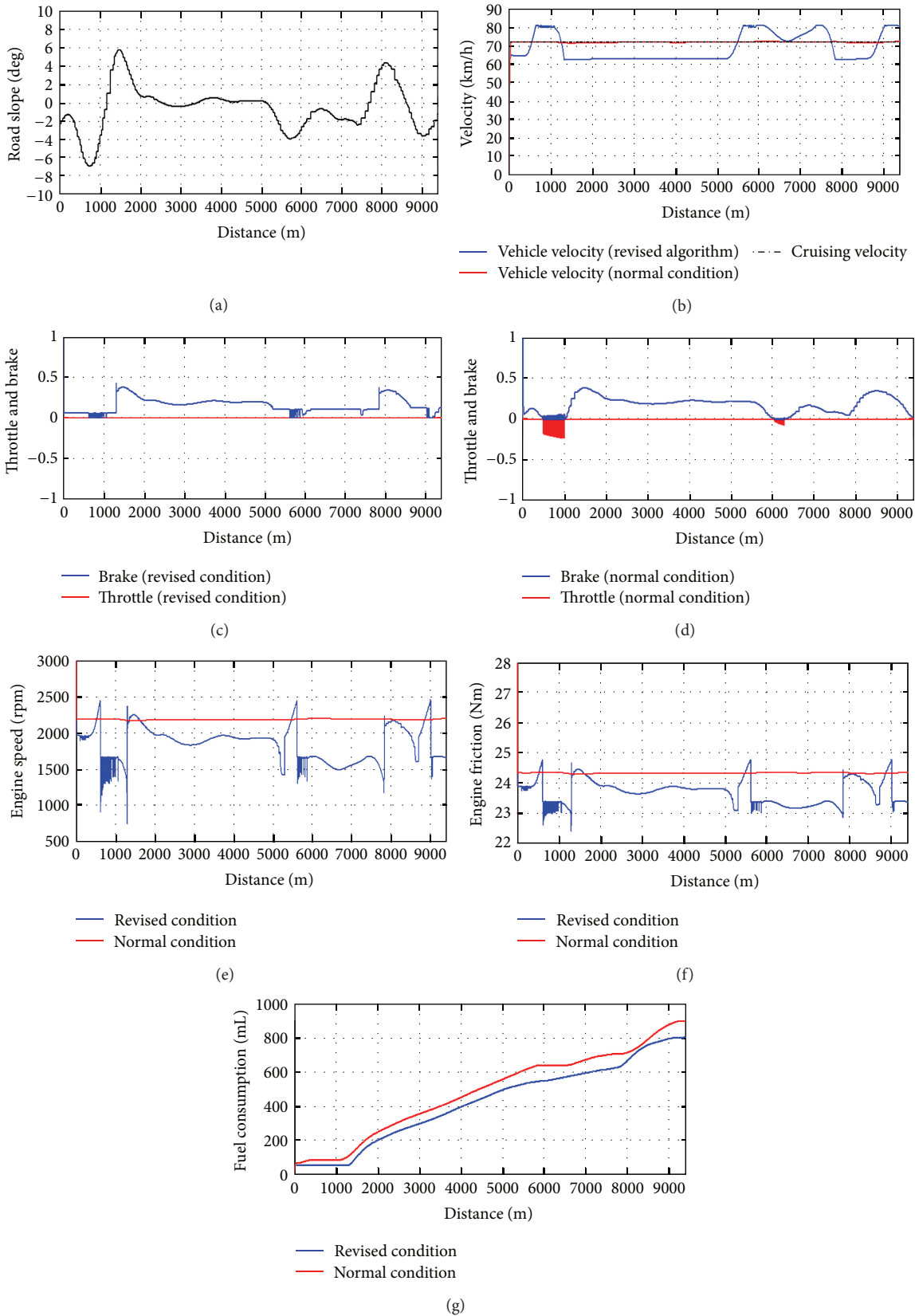


FIGURE 8: (a) Road slope. (b) Velocity obtained with and without revised algorithm. (c) Control action resulted from revised condition. (d) Control action resulted from normal condition, (e) comparison of the engine speeds. (f) Comparison of the engine frictions, and (g) comparison of the fuel consumptions obtained for two conditions.

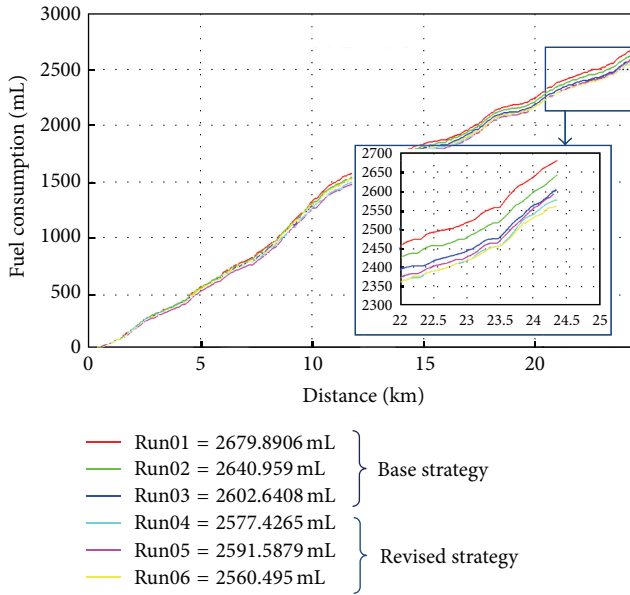


FIGURE 9: The accumulated fuel used versus the vehicle distance travelled.

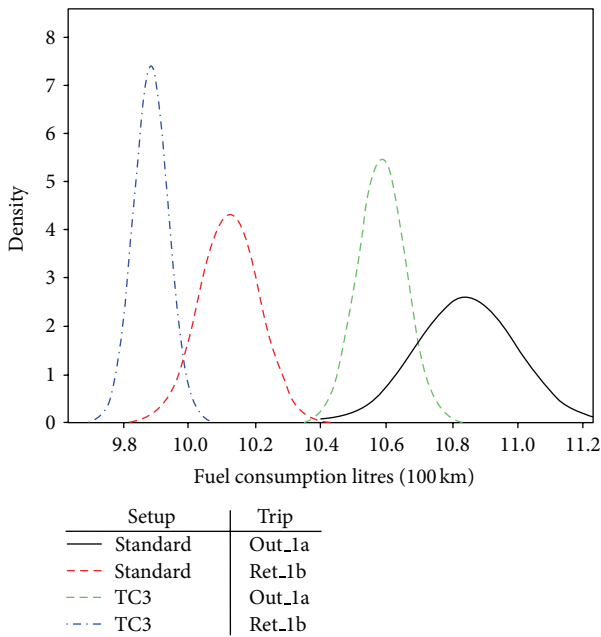


FIGURE 10: The histogram of measured fuel consumption (litres/100 km) for two different journeys called “Out_1a” & “Ret_1a”, with standard and revised (TC3) strategies.

with only using the throttle. After running the simulation, the profile of throttle opening depicted in Figure 7(c) is obtained. Then, the simulation is run by using the same profile of throttle opening as an input to the vehicle model but without utilizing the CC algorithm. The same results as those obtained using the CC, that is, the vehicle velocity follows the cruising velocity, are expected and achieved. The throttle opening obtained from this test (see Figure 7(c)) is zero within two distances (from 475 to 800 m and from 1600 to 1950 m).

5.1.2. Coasting with Revised Algorithm. This test is implemented to investigate the influence of the revised algorithm on the fuel consumption. Here, the same profile of throttle opening as that obtained from previous test is used but assuming that when the throttle is closed, the revised algorithm gets activated during the coasting phase of the vehicle. Activating the revised algorithm results in getting less loss for the time periods when the throttle is closed. Therefore, the constant speed will not be maintained but rather the speed of the vehicle will go up slightly; however, we can get the reduction of fuel consumption. The results demonstrate (Figure 7(d)) that a reduction in fuel consumption of 12% can be achieved by using the revised algorithm.

5.1.3. Cruise Control (CC) including Dead Zone and the Revised Algorithm. Based on the previous test, it can be realized that the saving can be obtained by allowing the speed to change; that is, cruising velocity will not be maintained constant. Therefore, we run the algorithm in which it is assumed that speed is not maintained perfectly but there is the dead zone (1.5 m/s) with speed. In this test, the cruise control together with the revised algorithm is utilized. As it is illustrated in Figure 7(c), introducing the dead zone while using the revised algorithm causes the throttle to remain closed for longer periods of time. In this case, fuel consumption is reduced as much as 20% (see Figure 7(d)).

5.2. Real Road-Map Profile. To carry out the realistic test, the road slope map recorded through a global positioning system (GPS) in Munich-Germany is used. The road profile used for the test is defined according to the road slope shown in Figure 8(a). In order to perform this test, a cruise control algorithm is utilized to follow the constant set-point speed (72 km/h) and it is carried out for the two following cases.

5.2.1. Cruise Control without Revised Algorithm. In this case, both the throttle and brake are controlled, as illustrated in Figure 8(d), in order to maintain the set-point speed (Figure 8(b)), that is, the cruising velocity. Contrary to the test carried out using the simulated road profile (Figure 7), here the brake is not zero because the slope of the real road-map profile is greater than in the simulated case.

5.2.2. Cruise Control (CC) with Revised Algorithm. Here, the revised algorithm is employed and constraint is introduced on the velocity which allows the vehicle velocity to go higher/lower than the cruising velocity rather than following the constant velocity. In this condition, the throttle opening only changes and the brake signal is maintained zero. During the time period when the throttle opening is zero (Figure 8(c)), the revised algorithm can be activated which causes the engine friction to decrease (Figure 8(f)) as the result of low engine speed (Figure 8(e)). The lower engine friction causes fuel consumption to decrease (Figure 8(g)).

Here, fuel consumption is reduced up to 12% through the revised condition. The fact that the vehicle does not have to always track a fixed cruising velocity helps to mitigate the loss of energy due to braking. It also allows the vehicle

to increase speed (Figure 8(b)) when going downhill which enables the vehicle to store more potential energy to cope with travelling uphill without having to consume so much fuel. Furthermore, in this condition the throttle can be closed for longer period which causes the revised algorithm to be activated and consequently engine friction to decrease.

6. Real Implementation

Some real tests have also been implemented in a vehicle utilising the revised strategy. This testing was conducted on a Range Rover Sport (Figure 4). The transmission torque converter control was modified to replicate the strategy. The testing is limited, but does show a statistically significant improvement in fuel economy. This modification was not optimal, and significant additional improvements in fuel consumption will be possible with an optimal controller in place. The results of the testing are shown in Figure 9. The plot shows the accumulated fuel used versus the vehicle distance travelled. The plots indicated by Run01 to Run06 were all captured from driving the vehicle on the identical route with similar traffic conditions, and there were no special driving styles adopted. However, there were the small variations in driver style and traffic. The plots depicted for Run01 to Run03 are for the tests for the base strategy, that is, does not use the revised strategy, while those depicted from Run04 to Run06 are for the tests when the revised strategy is used.

Figure 10 shows a histogram of data for two different journeys, called "Out_1a" & "Ret_1a", with standard and revised (TC3) strategies. Each journey is repeated several times with the original and new revised control system. The curves show the variation in measured fuel consumption (litres/100 km) used for each of these journeys and each control system. For example, journey "Ret_1b" has an average of 10.12 litres/100 km fuel consumption with original strategy, and new strategy achieves 9.89 litres/100 km. The data was analysed to confirm that this improvement was statistically significant (i.e., the separation between the curves is greater than test to test variability).

7. Conclusions

In this paper, the feasibility study on the fuel efficiency during coasting was carried out through the simulation. Both locked-up and unlocked-up modes of the torque converter and the switching between these two modes of operation were investigated in the simulation. The accuracy of the integrated simulation model of the longitudinal vehicle dynamics was validated by comparing the results against the Jaguar Land Rover (JLR) data. The paper has presented modeling of the following situations:

- (i) vehicle coasting down on the flat-road with the torque converter locked-up (in normal operating mode),
- (ii) vehicle coasting down on the flat-road with the torque converter unlocked-up,
- (iii) to present a realistic scenario, the tests have been implemented on the inclined road. These tests have

been carried out by utilizing the simulated road profile (sinusoidal inclination) and a real road profile, which is used to emulate a real-world drive cycle, with and without using the revised algorithm.

In all above cases, two virtual PID controllers have been utilized to keep the engine idle speed depending on the vehicle speed and throttle opening position. As a result of simulation investigation, longer coasting duration can be achieved or less fuel can be consumed through reducing the engine speed. Reduction of the engine speed can be achieved by controlling the torque converter operation which is called as the revised algorithm in this paper. Therefore, incorporating the revised algorithm in the typical power-train system increases the fuel economy saving. The test results indicated that the coasting by employing the revised algorithm could reduce fuel consumption and increase the travelled distance. The results have demonstrated that fuel consumption can be reduced about 7.9% through the proposed approach when the vehicle coasts on the flat road. In other word, the travelled distance could increase about 17.14%, that is, the longer coast duration. Fuel saving can be increased up to 12% when coasting on the inclined road. The losses in the torque converter during reengaging the engine over the repeated costing/acceleration schedule will have only a small effect in the overall fuel consumption value, since the total time elapsed during this phase is relatively small compared to the whole drive cycle. Of course, further work will be undertaken to assess all efficiencies and other factors in more detail, which will be subject of future research. Unconstrained vehicle speed increases during cruise control coasting would not be suitable for production. Some balance between speed deviation and fuel economy would need defining. Furthermore, even with no speed deviation, a fuel economy benefit is realized due to longer coast duration. In order to take the most advantage of the revised algorithm, the optimal velocity trajectory for a particular road profile needs to be calculated by utilizing a suitable algorithm such as dynamic programming (DP) and Pontryagin's Minimum Principle. This investigation would be carried out in the future research work.

Appendix

A. Derivation of the Vehicle Simulation Model

A.1. Powertrain Model. Figure 11 shows the schematic diagram of a power-train which demonstrates the transmission of the torque and velocity from the engine to the wheels. The automatic transmission is considered in the power-train model. Therefore, the torque produced by the engines is transmitted to the gear box through the torque converter [17–19]. The torque converter consists of three essential parts, that is, the impeller, the turbine, and the reactor. The impeller is connected to the crankshaft that transmits the power of the engine to the turbine through the hydraulic oil inside the torque converter. In turn the turbine is connected to the output shaft of the converter which is coupled to the input shaft of the gear box. The torque getting through the gear

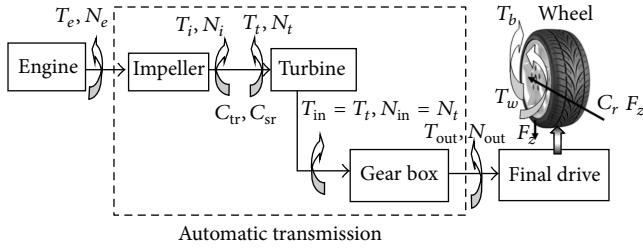


FIGURE 11: Schematic diagram of the powertrain, demonstrating the transmission of the torque and velocity from the engine to the wheels.

box varies depending on the gear ratio. Finally the output torque from the gear box is transmitted to the wheels after passing through the final drive. The torque and rotation speed of the wheel are affected by the brake torque and the external forces exerted on the vehicle including rolling resistance force resulted from the interaction between the tyre and the road, gravitational force, and aerodynamic drag force. The powertrain model is simulated by considering the two states of the torque converter-locked and unlocked states.

A.1.1. Model Presenting Unlock State of the Torque Converter. If the torque converter is unlocked-up, the torque produced via engine is transmitted by the fluid flowing through the impeller, turbine, and stator; this is the so-called fluid coupling. In order to develop the simulation model which presents unlocked state of the torque converter, the interaction between the engine and the torque converter must be taken into consideration. The engine model corresponding to the unlocked state of the torque converter can be defined by following equation [15, 20]:

$$I_{ei}\dot{N}_e = T_{eb}, \quad (\text{A.1})$$

where N_e denotes the engine rotation speed (rpm), I_{ei} denotes the summation of moment of inertia of the engine and the impeller, and T_{eb} denotes the engine brake torque which is determined by considering all the losses in the engine as follows:

$$T_{eb} = T_{ei} - T_f - T_p - T_l, \quad (\text{A.2})$$

where T_{ei} denotes the engine indicated torque, which depends both on the value of the engine rotation speed (N_e) and the throttle opening position (u_t) within the range $[0, 1]$. T_f and T_p denote, respectively, the friction loss and pumping loss (for brevity in this paper, these two terms are lumped and denoted by the engine friction). T_l indicates the additional acting load on the engine and here, the impeller torque (T_i) is only considered as an additional acting load on the engine; that is, $T_l = T_i$.

The engine model determined by the above equations together with the two PID controllers explained in Section 3 presents Engine 1, illustrated in Figure 4. The engine indicated torque, and the engine friction are obtained by using two look-up tables in the simulation. The value of the engine friction depends on the engine rotation speed and air mass flow.

The magnitudes of the impeller torque and throttle opening are acquired by the switching algorithm (see Figure 4).

Parameters playing an important role in the performance of a torque converter are the speed ratio ($C_{sr} = w_t/w_i$), the torque ratio ($C_{tr} = T_t/T_i$), the efficiency ($\eta_e = C_{tr}C_{sr}$), and the capacity factor or K -factor (K_{tc}), where T_i is the impeller torque (converter input torque), w_i is the impeller speed (converter input speed), T_t is the turbine torque (converter output torque), and w_t is the turbine speed (converter output speed). The capacity factor shows the ability of the converter to absorb or transmit the torque [17, 21].

By assuming that the impeller speed (N_i) is identical to the engine speed (N_e), the impeller torque can be obtained as follows:

$$T_i = \left(\frac{N_e}{K_{tc}} \right)^2. \quad (\text{A.3})$$

Knowing the torque ratio (C_{tr}) and speed ratio (C_{sr}) enables us to calculate the turbine torque as follows:

$$T_t = C_{tr}T_i. \quad (\text{A.4})$$

The torque ratio (C_{tr}) and K -factor (K_{tc}) can be interpolated from the torque converter characteristic maps against the speed ratio (C_{sr}) [3]. These maps are depicted in Figure 12. By neglecting distortion and damping effect of the rotating part, the turbine torque and its speed will be identical to input torque (T_{in1}) and input speed (N_{in}) of the transmission. T_{in1} indicates the transmission input torque while the torque converter is unlocked.

A.1.2. Model Presenting Locked-Up State of the Torque Converter. Considering the torque converter to be locked up, the engine torque and its speed will be entirely transmitted to gear box input shaft; therefore, the torque converter can be disregarded in the equations presenting that condition. The equation presenting locked-up state of the torque converter is determined as follows:

$$I_{et}\dot{N}_e = T_{ei} - T_f - T_p - T_{in2}, \quad (\text{A.5})$$

where N_e denotes the engine rotation speed (rpm). I_{et} denotes the summation of moment of inertia of the engine, torque converter, and gear box. T_{ei} denotes the engine indicated torque. T_f and T_p denote the friction and pumping losses, respectively. T_{in2} denotes the transmission input torque while torque converter is locked. By neglecting distortion and damping effect of the rotating part, the engine speed (N_e) will be identical to the transmission input speed (N_{in}). Therefore, the transmission input torque (T_{in2}) can be calculated as follows:

$$T_{in2} = T_{ei} - T_f - T_p + I_{et}\dot{N}_{in}. \quad (\text{A.6})$$

The engine indicated torque (T_{ei}) and friction (T_f) and pumping (T_p) losses are obtained from the same lookup tables as those used for the unlocked state of the torque converter, however, here the transmission input speed (N_{in})

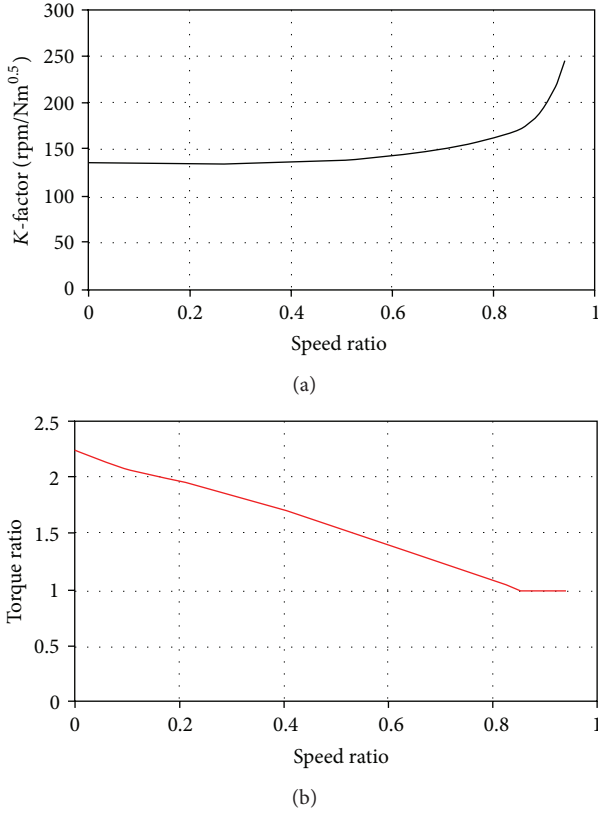


FIGURE 12: Performance characteristic of a torque converter—(a) K -factor and (b) torque ratio.

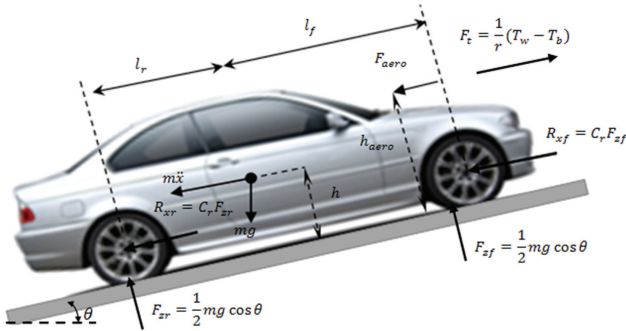


FIGURE 13: Exerting forces on the vehicle during travelling on inclined road.

is used in place of the engine speed (N_e) in the interpolation. (A.6) presents Engine 2, depicted in Figure 2.

Transition may occur between the two states of the torque converter; locked and unlocked states. This transition is implemented through a switching algorithm in the simulation. For normal condition, the switch is only triggered according to the velocity of the vehicle. Therefore, the torque coveter is locked-up at the speed higher than 17.88 m/s, and subsequently the model presented by (A.6) is utilized.

A.1.3. Common Elements in the Power-Train Model for Locked and Unlocked States of the Torque Converter. The torque and

rotation speed transmitted to the wheel through gear box and the final drive can be obtained as follows:

$$\begin{aligned} T_w &= R_{tr} R_{fd} T_{in}, \\ N_w &= \frac{N_{in}}{R_{tr} R_{fd}}, \end{aligned} \quad (\text{A.7})$$

where T_{in} and N_{in} are the torque and the speed on the input side of the transmission, respectively. R_{tr} and R_{fd} are the gear ratio and the final drive ratio, respectively. T_w and N_w indicate the torque and rotation speed of the wheel.

A.2. Brake Model. The torque generated by the brake system can be obtained by the following equation [22, 23]:

$$T_b = K_b P_b, \quad (\text{A.8})$$

where K_b denotes the lumped gain for entire brake system and P_b , the amount of pressure produced behind the brake disk. This pressure is described by the following dynamic equation:

$$P_b = 150 K_c u_b - \tau_b P_b, \quad (\text{A.9})$$

where K_c denotes the brake pressure gain, τ_b the lumped lag obtained by combining two lags relating to the dynamics of the servo valve and the hydraulic system, and u_b is the brake pedal position within the range $[-1, 0]$.

A.3. Vehicle Dynamics Model. Utilizing the second Newton's law which takes balancing of the forces exerted on the vehicle consisting of rolling resistance force (R_z), aerodynamic force (F_{aero}), gravitational force (F_g) and the forces generated on the wheel by the brake torque (T_b) and the engine torque (T_w) (Figure 13), the acceleration of the vehicle (a) can be obtained as follows:

$$Ma = \frac{1}{r} (T_w - T_b) - \frac{\frac{1}{2} \rho A C_d v^2}{F_{aero}} - \frac{C_r mg \cos(\theta)}{R_z} - \frac{mg \sin(\theta)}{F_g}. \quad (\text{A.10})$$

Here ρ denotes the air density, r the wheel radius, C_r the rolling resistance coefficient, C_d the drag coefficient which depends on the vehicle's body shape, v vehicle velocity, A the frontal cross area of the vehicle, and g the gravitational acceleration. θ indicates the road slope. In order to take into account the effect of rotating part on the vehicle dynamics, the moment of inertial of the wheels has to be lumped with the vehicle mass:

$$M = \frac{n_w I_w}{r^2} + m, \quad (\text{A.11})$$

where I_w denotes the moment of inertia of a wheel, n_w indicates the number of the wheels, m the mass of the vehicle, and r the wheel radius. Consequently By integrating the acceleration, the velocity of the vehicle will be obtained. The values of the parameter used in the equation are given in Table 1.

TABLE 1: Values of the parameters used in the equations.

Parameter	Description	Numerical value
m	Vehicle mass	2270 [kg]
r	Wheel radius	0.326 [m]
R_{tr}	Gear ratio	3, 2.34, 1.85, 1.45, 1.00, 0.68
R_{fd}	Final driver ratio	3.28
I_{ei}	Moment of inertia of engine and torque converter	0.224 [kgm ²]
I_{et}	Moment of inertia of engine, torque converter and transmission	0.226 [kgm ²]
I_w	Moment of inertia of the wheel	1.7 [kgm ²]
$\rho \cdot A \cdot c_d$	Aerodynamic force coefficient	1.2 [kg/m]
C_r	Rolling resistance coefficient	0.015
n	Engine stroke	4
V_d	Engine displacement volume	0.005 [m ³]
g	Gravitational acceleration	9.8 [m/s ²]
τ_b	Lumped lag-servo valve and the hydraulic system	0.2
K_c	Pressure gain	1
K_b	Lumped gain for entire brake system	20 [Nm/bar]
n_w	Number of the wheels	4

Abbreviations

A : Frontal cross-section area of the vehicle
 C_d : Aerodynamic drag coefficient
 C_r : Rolling resistance coefficient
 C_{sr} : Speed ratio
 C_{tr} : Torque ratio
 F_{aero} : Aerodynamic force
 F_g : Gravitational force
 g : Gravitational acceleration
 I_{ei} : Summation of moment of inertia of the engine and the impeller
 I_{et} : Summation of moment of inertia of the engine, torque converter, and gear box
 I_w : Moment of inertia of a wheel
 K_b : Lumped gain for entire brake system
 K_c : Brake pressure gain
 K_{tc} : Capacity factor or K -factor
 m : Mass of the vehicle
 n : Engine stroke
 N_e : Engine rotation speed
 N_i : Impeller speed
 N_{in} : Transmission input speed
 N_t : Turbine torque
 N_w : Wheel rotation speed
 n_w : Number of the wheels
 P_b : Pressure behind the brake disk
 r : Wheel radius
 R_{fd} : Final drive ratio
 R_{tr} : Gear ratio
 R_z : Rolling resistance force
 T_b : Brake torque
 T_{eb} : Engine brake torque
 T_{ei} : Engine indicated torque
 T_f : Friction loss
 T_i : Impeller torque
 T_{ic} : Impeller torque calculated by PID controller

T_{in} : Transmission input torque
 T_{in1} : Transmission input torque while torque converter is locked
 T_{in2} : Transmission input torque while torque converter is unlocked
 T_{is} : Impeller torque from switching algorithm
 T_l : Acting load
 T_p : Pumping loss
 T_t : Turbine torque
 T_w : Wheel torque
 u_b : Brake pedal position
 u_t : Throttle opening position
 u_{tc} : Throttle opening calculated by PID controller
 u_{ts} : Throttle opening from switching algorithm
 v : Vehicle velocity
 τ_p : Lumped lag-servo valve and hydraulic system
 a : Vehicle acceleration
 θ : Road slop
 ρ : Air density.

Conflict of Interests

The authors do not have any financial relationship with the company Mathworks (MATLAB software).

Acknowledgments

The authors would like to thank Peter Kock from the Central Engineering Division of MAN (Truck & Bus) Nutzfahrzeuge AG in Munich, Germany, for providing the real road-map profile. This work has been carried out as a collaborative project between Kingston University of London and Jaguar Land Rover (JLR) in the UK.

References

- [1] J. Barrand and J. Bokar, "Reducing tire rolling resistance to save fuel and lower emissions," *SAE International Journal of Passenger Cars*, vol. 1, no. 1, pp. 9–17, 2009.
- [2] H. D. Tarpinian, G. H. Nybakken, and J. Mishory, "A fuel saving passenger tire," *SAE Technical Paper*, no. 790726, 1979.
- [3] D. Y. Lee, H. H. Ju, J. S. Rhee, S. H. Lee, and H. S. Lee, "Adaptive anti-shock coasting lock-up control of the torque converter clutch," *World Academy of Science, Engineering and Technology*, vol. 15, pp. 97–102, 2006.
- [4] J. Lee, *Vehicle Inertia Impact on Fuel Consumption of Conventional and Hybrid Electric Vehicle Using Acceleration and Coast Driving Strategy [Ph.D. thesis]*, Virginia Polytechnic Institute and State University, Blacksburg, Virginia, USA, 2009.
- [5] T. van Keulen, G. Naus, B. de Jager, R. van de Molengraft, M. Steinbuch, and E. Aneke, "Predictive cruise control in hybrid electric vehicles," *World Electric Vehicle Journal*, vol. 3, no. 1, 2009.
- [6] T. Van Keulen, B. De Jager, D. Foster, and M. Steinbuch, "Velocity trajectory optimization in Hybrid Electric trucks," in *Proceedings of the American Control Conference (ACC '10)*, pp. 5074–5079, Marriott Waterfront, Baltimore, Md, USA, July 2010.
- [7] A. Rousseau, S. Pagerit, and D. W. Gao, "Plug-in hybrid electric vehicle control strategy parameter optimization," *Journal of Asian Electric Vehicles*, vol. 6, no. 2, pp. 1125–1133, 2008.
- [8] D. Sinoquet, G. Rousseau, and Y. Milhau, "Design optimization and optimal control for hybrid vehicles," *Optimization and Engineering*, vol. 12, no. 1-2, pp. 199–213, 2011.
- [9] E. Hellstrom, *Explicit use of road topography for model predictive cruise control in heavy truck [M.S. thesis]*, Linkopings universite, Linkopings, Sweden, 2005.
- [10] E. Hellström, M. Ivarsson, J. Åslund, and L. Nielsen, "Look-ahead control for heavy trucks to minimize trip time and fuel consumption," *Control Engineering Practice*, vol. 17, no. 2, pp. 245–254, 2009.
- [11] E. Kozica, *Look Ahead Cruise Control: Road Slope Estimation and Control Sensitivity [M.S. thesis]*, Master's Degree Project, Stockholm, Sweden, 2005.
- [12] P. Kock, H.-J. Welfers, B. Passenberg, S. Gnatzig, O. Stursberg, and A. W. Ordys, "Saving energy through predictive control of longitudinal dynamics of heavy trucks," *VDI Berichte*, no. 2033, pp. 53–67, 2008.
- [13] N. Muller, S. Straub, S. Tumback, and A. Christ, "Coasting-next generation start/stop systems," *MTZ*, vol. 72, no. 9, pp. 14–19, 2011.
- [14] P. Shakouri, A. Ordys, M. Askari, and D. S. Laila, *Longitudinal Vehicle Dynamics Using Simulink/Matlab*, UKACC International conference on CONTROL, Coventry, 2010.
- [15] J. B. Heywood, *Internal Combustion Engine Fundamentals*, McGraw-Hill, 1988.
- [16] P. Shakouri, A. Ordys, and D. S. Laila, "Adaptive cruise control system: comparing gain-scheduling PI and LQ controllers," in *Proceedings of the 18th IFAC World Congress*, Milano, Italy, August 2011.
- [17] J. Y. Wang, *Theory of Ground Vehicle*, Wiley-IEEE, 3rd edition, 2001.
- [18] D. Geuns, *Description Automatic Transmission VTIF*, ZF Getriebe Sint-Truiden, 2003.
- [19] C. H. Yao, *Automotive Transmissions: Efficiently Transferring Power from Engine to Wheels*, Discovery Guides, Pro Quest, 2008.
- [20] H. Heisler, *Advanced Vehicle Technology*, College of North West London, 2nd edition, 2002.
- [21] MathWorks, *Using Simulink and Stateflow in Automotive Application*, Automatic transmission control, 1998.
- [22] M. Short, M. J. Pont, and Q. Huang, *Simulation of Vehicle Longitudinal Dynamic*, Embedded System Laboratory University of Leicester, safety and reliability of Distributed Embedded Systems, Leicester, 2004.
- [23] J. C. Gerdes and J. K. Hedrick, "Vehicle speed and spacing control via coordinated throttle and brake actuation," *Control Engineering Practice*, vol. 5, no. 11, pp. 1607–1614, 1997.

